scientific reports

Check for updates

OPEN

Study on the predictive value of preoperative CT features for the mitotic index of GIST based on the nomogram

Ren Yingzheng, Jiang Linlin, Yang Yang, An Junjie & Dong Yonghong✉

This study aimed to construct a Nomogram based on preoperative CT features to predict the mitotic index in gastrointestinal stromal tumors and to establish preoperative risk stratification. The constructed nomogram prediction model is targeted towards guiding preoperative risk stratification, facilitating the provision of rational drug administration regimens, and tailoring appropriate surgical plans for personalized treatment. The imaging and pathological data of 250 patients with gastrointestinal stromal tumors in Shanxi Provincial hospital from January 2019 to January 2024 were retrospectively analyzed. According to the pathological data, the patients were divided into high mitotic index and low mitotic index, and were divided into a training group ($n = 176$) and a validation group ($n = 74$) according to a stratified sampling ratio of 7:3. In the training group, statistically significant variables were screened out by univariate analysis for multivariate logistic regression analysis, and independent risk factors were screened out and a Nomogram prediction model was constructed. The receiver operating characteristic (ROC) was used to evaluate the model discrimination, and the predicted probability risk was stratified by the optimal cutoff value. The Hosmer-Lemeshow test (HL test) was performed, and the calibration curve was drawn by Bootstrap repeated sampling 1000 times to evaluate the model consistency. Finally, the clinical application value of the prediction model was evaluated by the decision curve analysis (DCA). There were no significant differences in the distribution of clinical characteristics and CT features between the training group and the validation group ($P>0.05$). Univariate analysis showed that the differences in tumor size, tumor site, boundary, calcification, liquefaction/necrosis, morphological characteristics, growth pattern, and ulceration were statistically significant ($P<0.05$). Multivariate logistic regression analysis screened out tumor size (GIST ≤ 2 cm, $P = 0.018$; GIST 2–5 cm, $p = 0.009$; GIST 5–10 cm, $P = 0.017$), liquefaction/necrosis ($P = 0.002$), and morphological characteristics ($P = 0.002$) as independent risk factors for high mitotic index. The Nomogram was established based on these three factors. The area under the curve (AUC) of the training group and the validation group of the model were 0.851 (95%CI: 0.793–0.91) and 0.836 (95%CI: 0.735–0.937), the specificity was 0.696 and 0.735, and the sensitivity was 0.869 and 0.760, respectively. The HL test had good calibration (training group $P = 0.461$, validation group $P = 0.822$), indicating that the predicted risk was consistent with the actual risk. The DCA also showed good clinical practicality. The Nomogram prediction model that incorporates preoperative CT features of tumor size, liquefaction/necrosis, and morphological characteristics can effectively predict the number of mitotic figures in gastrointestinal stromal tumors, and can perform effective preoperative risk stratification to guide clinical decision-making and personalized treatment.

Gastrointestinal stromal tumors (GIST) are potentially malignant sarcomas originating from interstitial Cajal cells and are the most common mesenchymal tumors of the gastrointestinal tract[1]. Globally, there are 6 to 22 patients with GIST per million people, and the clinical manifestations can be diverse, primarily including abdominal pain, indigestion, anemia, bleeding, and other symptoms[2,3]. The primary treatment for localized GIST is radical surgical resection. However, despite this, approximately 30–40% of patients with intermediate to high

Department of Gastroenteropancreatic & Hernia Surgery, Shanxi Provincial People's Hospital, Shanxi Medical University, Shanxi 030012, China. ✉email: youthdong007@163.com

risk experience metastasis and recurrence following surgery, significantly impacting their prognosis[4]. Studies have demonstrated that neoadjuvant imatinib exhibits positive outcomes in assisting patients with intermediate to high-risk GIST in achieving R0 resection and reducing the risk of postoperative recurrence[5,6]. Therefore, accurate preoperative risk stratification is of paramount importance. The National institutes of health(NIH) criteria indicate that tumor size and mitotic index are two crucial indicators for predicting malignant potential and guiding stratification[7]. The mitotic index serves as an independent risk factor for assessing postoperative recurrence in GIST[8]. However, currently, the acquisition of mitotic index primarily relies on postoperative pathological examination. While preoperative biopsy can provide mitotic index, it increases the risk of tumor rupture and dissemination[9]. Therefore, a preoperative method to predict mitotic index is crucial for guiding risk stratification and personalizing treatment plans. CT, being a routine and non-invasive diagnostic tool for GIST, readily provides valuable information on superficial features including size, location, margins, calcification, ulceration, liquefaction/necrosis, morphological patterns, and growth modalities, which can potentially contribute to the prediction of mitotic index. In this study, we retrospectively analyzed CT features to identify risk factors predictive of high mitotic index in GIST. This study aimed to construct a Nomogram based on preoperative CT features to predict the mitotic index in GIST and to establish preoperative risk stratification. The constructed nomogram prediction model is targeted towards guiding preoperative risk stratification, facilitating the provision of rational drug administration regimens, and tailoring appropriate surgical plans for personalized treatment.

Materials and methods
Ethical approval
The study was approved by the Ethics Committee of Shanxi Provincial People's Hospital affiliated to Shanxi Medical University, with a waiver of the requirement for informed consent. This research was conducted in accordance with the ethical standards outlined in the Declaration of Helsinki of 1964 and its later amendments or comparable ethical standards. The Institutional Review Board (IRB) granted a waiver for written informed consent. Approval from the IRB has been obtained.

General information
A retrospective analysis was conducted on 250 patients with GIST who underwent preoperative CT examination and surgical treatment at Shanxi Provincial People's Hospital between January 2019 and January 2024. Inclusion Criteria: (1) Patients who underwent initial surgical resection of the primary tumor at Shanxi Provincial People's Hospital; (2) Postoperative resected specimens underwent consecutive tissue sectioning and immunohistochemical staining, with postoperative pathology confirming the diagnosis of GIST; (3) Abdominal CT scan with plain and enhanced imaging performed within 15 days prior to surgery at our hospital, with Omnipaque used as the contrast agent for some patients and Ultravist for the remainder; (4) Complete and accessible clinical data, imaging data and reports, as well as pathological information of the patients. Exclusion Criteria: (1) Patients with preoperative diagnosis of primary tumor metastasis; (2) Patients with a history of previous GIST surgical resection and a current diagnosis of postoperative recurrence; (3) Preoperative diagnosis of multiple foci or concurrent presence of other types of malignant tumors in the gastrointestinal tract; (4) Patients with tumor rupture during surgery or preoperative period; (5) Patients who received other forms of treatment before surgery, such as radiotherapy, chemotherapy, targeted therapy, etc. A total of 250 patients were included and stratified by a 7:3 ratio into a training group (176 patients) and a validation group (74 patients) using stratified sampling methods.

CT imaging techniques
The examination was conducted using a Philips Brilliance 256-slice CT scanner, an ultra-fast model provided by Philips. The scanning parameters were as follows: tube voltage of 120 kV, tube current of 250 mA, slice thickness and interval both at 5 mm, matrix size of 512×512, and window width for the plain scan sequence ranging from 250 to 300 HU (Hounsfield Units), with a window level at 30–50 HU. After the CT plain scan, a high-pressure injector administered 80.0 ml of contrast agent, either Omnipaque or Ultravist, via the median cubital vein at a rate of 3.5 ml/s. The imaging characteristics of GIST were independently assessed by two readers with 5 and 10 years of experience in abdominal imaging, respectively, in a blinded manner. In cases where discrepancies in imaging features were observed, the two readers re-evaluated the images and reached a consensus.

Patient selection
Clinical data were collected from all patients, including gender and age, CT features were analyzed, focusing on: (1) Tumor site, including stomach, non-stomach (such as duodenum, jejunum, ileum, colon, rectum, esophagus, etc.); (2) Boundaries, including clear and unclear; (3) Calcification: A gastric density measurement exceeding 120 HU serves as an indication of calcification. (4) Tumor size: The maximum diameter of the tumor was measured in the axial, coronal, and sagittal planes of the image. The average of the two maximum values was taken as the maximum diameter of the tumor. The measurement unit was mm. The tumor size was divided into ≤ 2 cm, 2–5 cm, 5–10 cm, and > 10 cm[10]. (5) Liquefaction/necrosis: liquefaction is manifested by a density of -20 to 20 HU in the measured area on plain scan images, and both liquefaction and necrosis are manifested as no enhancement in enhanced images; (6) Morphological characteristics, including regular shape (smooth edges, round or oval) and irregular shape (lobed edges, uneven); (7) The growth patterns include intraluminal growth (attached to the intestinal wall and confined within the lumen), extraluminal growth (confined to the extraluminal space), and mixed growth (exhibiting characteristics of both endophytic and exophytic growth); (8) Ulcers, characterized by an uneven surface of the lesion, local tissue discontinuity, and a large defect area on the surface.

Pathological data: The risk of GIST was categorized into four grades based on the modified NIH 2008 criteria: very low, low, intermediate, and high risk. For the purpose of this study, very low, low, and intermediate risk were grouped together as low malignancy, while high risk was considered as high malignancy[11]. In addition, under the microscope, we select the areas where tumor cells are dense and have typical morphologies, and then determine the mitotic index in 50 high-power fields (HPF). Based on this, we divide the mitotic index of GIST into two groups: the low-mitotic-index group (≤ 5/50HPF) and the high-mitotic-index group (> 5/50HPF)[12,13].

Statistical analysis

Statistical analysis was performed using SPSS 25.0. The provided data were stratified into a training set and a validation set in a 7:3 ratio based on the outcome variable, mitotic index. Differential analysis was conducted on the training and validation sets to examine whether continuous variables followed a normal distribution. For variables that adhered to a normal distribution, the T-test was employed, whereas the Mann-Whitney U test was used for those that did not. For categorical variables, the Chi-square test was applied when the total sample size was ≥ 40 and the expected frequency was ≥ 5; otherwise, the Fisher's exact test was used. Descriptive statistical analyses were conducted separately on the data from the training set and the validation set, with mitotic index serving as the grouping variable. Statistical significance was considered at $P < 0.05$. For the analysis of influencing factors, logistic regression analysis was employed. Univariate logistic regression analysis was first conducted on the training set data to select variables that were significantly associated with the outcome ($P < 0.05$). These significant variables were then included in the multivariate logistic regression. The model was optimized through a stepwise regression approach to ultimately determine the most appropriate combination of variables. During the stepwise regression process, variable selection was based on criteria including statistical significance, minimization of the Akaike Information Criterion (AIC), and support from domain knowledge. Based on the identified risk factors, a Nomogram was constructed using R4.3.0 software to calculate the risk scores for each factor. The model was evaluated using ROC curves, HL tests, calibration curves, and DCA. Risk stratification was performed based on the cutoff value derived from the ROC curve analysis, and a bar chart was constructed accordingly. Calibration curves were plotted through 1000 bootstrap resamples. The level of significance was set at α = 0.05.

Results

Clinical and CT characteristics

A total of 250 patients were enrolled and divided into a training group ($n = 176$) and a validation group ($n = 74$) in a 7:3 ratio. Comparison of clinical and CT characteristics between the two groups revealed no statistically significant differences in age, gender, tumor site, boundaries, calcification, tumor size, liquefaction/ necrosis, morphological characteristics, growth pattern, or Ulcers (all $P > 0.05$), indicating that the groups were comparable. The comprehensive findings are presented in Table 1.

Variables		Training cohort ($n = 176$)	Validation cohort ($n = 74$)	Statistic	P value
Age, y		60.05 (10.65)	59.50 (11.34)	0.362	0.717
Sex	Female	90 (51.1)	43 (58.1)	1.017	0.313
	Male	86 (48.9)	31 (41.9)		
Tumor site	Gastric	135 (76.7)	57 (77.0)	0.003	0.956
	Others	41 (23.3)	17 (23.0)		
Boundaries	Unclear	41 (23.3)	19 (25.7)	0.162	0.687
	Clear	135 (76.7)	55 (74.3)		
Calcification	No	129 (73.3)	62 (83.8)	3.178	0.075
	Yes	47 (26.7)	12 (16.2)		
Tumor size	> 10 cm	24 (13.6)	8 (10.8)	5.199	0.158
	≤ 2 cm	20 (11.4)	16 (21.6)		
	2–5 cm	93 (52.8)	32 (43.2)		
	5–10 cm	39 (22.2)	18 (24.3)		
Liquefaction/necrosis	No	109 (61.9)	52 (70.3)	1.58	0.209
	Yes	67 (38.1)	22 (29.7)		
Morphological characteristics	Irregular	67 (38.1)	24 (32.4)	0.715	0.398
	Regular	109 (61.9)	50 (67.6)		
Growth pattern	Mixed growth	32 (18.2)	18 (24.3)	1.528	0.466
	Intracavity growth	96 (54.5)	35 (47.3)		
	Exophytic growth	48 (27.3)	21 (28.4)		
Ulcers	No	105 (59.7)	53 (71.6)	3.205	0.073
	Yes	71 (40.3)	21 (28.4)		

Table 1. Clinical and CT characteristics.

Construction of prognostic model

According to the univariate logistic analysis, clinical data such as age and gender were not significantly related to the mitotic index in GIST ($P > 0.05$, Table 2), whereas CT characteristics including tumor location, boundaries, calcification, tumor size, liquefaction/necrosis, morphological characteristics, growth pattern, and ulcers were significantly associated ($P < 0.05$, Table 2).

After incorporating statistically significant factors from the univariate analysis into the multivariate logistic analysis, the results indicated that tumor size, liquefaction/necrosis, and morphological characteristics were independent risk factors for high mitotic index in GIST, as shown in Table 3. Specifically, GISTs with sizes ≤ 2 cm (OR = 0.083, 95%CI: 0.011–0.656, $P = 0.018$), 2–5 cm (OR = 0.14, 95%CI: 0.032–0.611, $P = 0.009$), and 5–10 cm (OR = 0.156, 95%CI: 0.034–0.717, $P = 0.017$) had significant protective effects on mitotic index compared to GISTs > 10 cm ($P < 0.05$). GISTs with liquefaction/necrosis (OR = 3.803, 95%CI: 1.615–8.955, $P = 0.002$) had a significant impact on mitotic index compared to those without liquefaction/necrosis, serving as an independent risk factor. Additionally, GISTs with regular morphology (OR = 0.233, 95%CI: 0.093–0.588, $P = 0.002$) had a significant protective effect on mitotic index compared to those with irregular morphology. A collinearity analysis was performed on the final model, and the variance inflation factor (VIF) > 10 was considered indicative of collinearity. However, the calculation results indicated no collinearity (VIF < 10).

Additionally, the HL test was employed to compare the differences between the predicted expected values and the observed values. The results demonstrated that there was no statistically significant difference between the predicted and observed values ($P > 0.05$, with $P = 0.461$ for the training set and $P = 0.822$ for the validation set). This finding suggests that the logistic model exhibits good fit, indicating that the model's predictions are in close agreement with the actual observations.

## Construction and validation of nomogram

Based on the statistically significant risk factors identified through logistic regression analysis, a Nomogram prediction model (Fig. 1) was constructed, where each patient's CT features correspond to an individual score. A total score is calculated from these CT features, with a higher total score indicating a higher number of

Variables	Standard error	Z value	P value	OR (95%CI)
Age, y	0.015	-0.756	0.450	0.989(0.960–1.018)
Sex				
Male	0.320	1.640	0.101	1.689(0.903–3.162)
Female*				
Tumor site				
Others	0.365	2.504	0.012	2.494(1.220–5.099)
Gastric*				
Boundaries				
Clear	0.371	-3.554	< 0.001	0.267(0.129–0.553)
Unclear*				
Calcification				
Yes	0.363	4.372	< 0.001	4.884(2.399–9.943)
No*				
Tumor size				
≤ 2 cm	0.968	-4.281	< 0.001	0.016(0.002–0.106)
2–5 cm	0.667	-4.860	< 0.001	0.039(0.011–0.145)
5–10 cm	0.696	-3.018	0.003	0.122(0.031–0.479)
> 10 cm*				
Liquefaction/necrosis				
Yes	0.369	6.340	< 0.001	10.353(5.027–21.324)
No*				
Morphological characteristics				
Regular	0.369	-6.340	< 0.001	0.097(0.047–0.199)
Irregular*				
Growth pattern				
Intracavity growth	0.434	-3.078	0.002	0.263(0.112–0.616)
Exophytic growth	0.457	0.183	0.855	1.087(0.444–2.660)
Mixed growth*				
Ulcers				
Yes	0.338	4.511	< 0.001	4.598(2.370–8.922)
No*				

Table 2. Univariate analysis of factors associated with the mitotic index of GIST. *Is the reference category.

Variables	Standard error	Z value	P value	OR	95%CI	VIF
Tumor size						
≤ 2 cm	1.055	-2.360	0.018	0.083	0.011–0.656	1.771
2–5 cm	0.751	-2.615	0.009	0.140	0.032–0.611	3.403
5–10 cm	0.778	-2.388	0.017	0.156	0.034–0.717	3.087
> 10 cm*						
Liquefaction/necrosis						
Yes	0.437	3.057	0.002	3.803	1.615–8.955	1.156
No*						
Morphological characteristics						
Regular	0.471	-3.089	0.002	0.233	0.093–0.588	1.346
Irregular*						

Table 3. Multivariate logistic regression analysis of factors associated with the mitotic index of GIST. *Is the reference category.
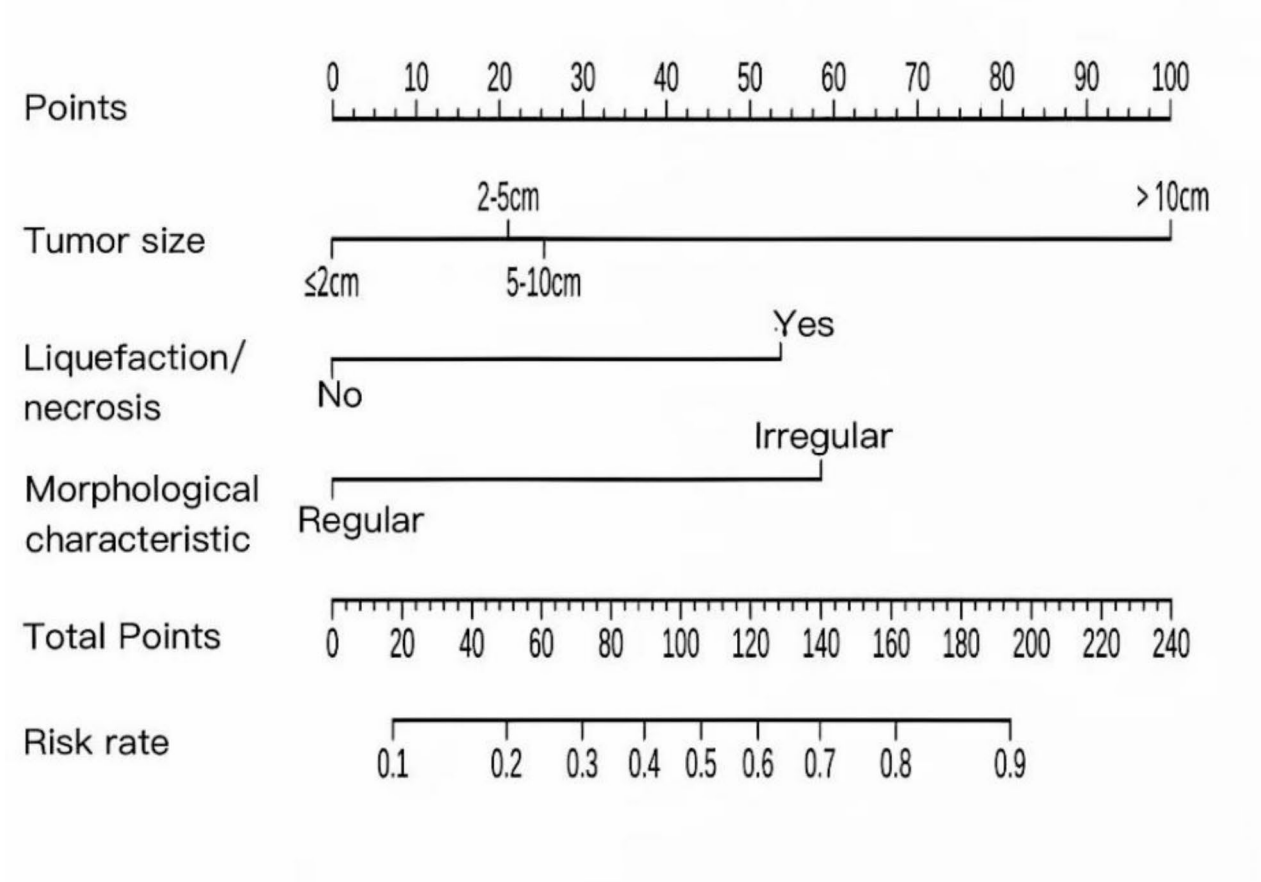
Fig. 1. Nomogram prediction model for GIST Mitotic index based on preoperative CT features.

mitotic index, thereby enabling a preliminary prediction of the postoperative pathological mitotic index based on preoperative CT features. In the training group, a nomogram model was established based on indicators such as tumor size, liquefaction/necrosis, and morphological characteristics. Specifically, the Points values corresponding to these indicators in the figure are added together to obtain the total score. Then, the total score is projected downward onto the Total points value in the figure, from which the predicted probability of GIST with a high mitotic index can be obtained (Figs. 1 and 2).The area under curve (AUC) for this model is 0.851 (95% CI: 0.793–0.91) (Fig. 3). The calibration curve exhibits an angle of inclination close to 45 degrees,
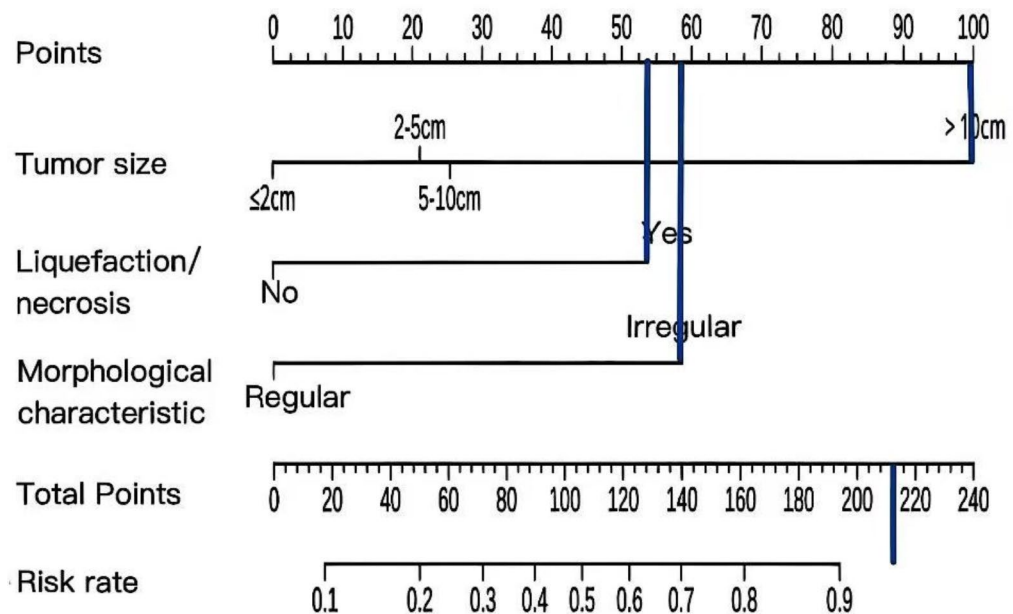
Fig. 2. Nomogram prediction model for GIST Mitotic index based on preoperative CT features.

indicating good consistency in predicting the number of mitotic index in GIST using preoperative CT features (Fig. 4). When the validation group data were applied to the Nomogram model, the results showed an AUC of 0.836 (95% CI: 0.735–0.937) (Fig. 3). The calibration curve closely aligns with the reference curve, indicating good consistency (Fig. 5).

Evaluation of model-based risk stratification and its clinical applicability

Based on the a cut-off value (sensitivity:0.869; specificity:0.696) of 0.226 (Youden Index: 0.565) from the ROC of the training group, the prediction model was divided into a high-risk group and a low-risk group (Fig. 6). For the validation group, based on the cut-off value of 0.226(Youden Index = 0.496) from the ROC, the prediction model was divided into a high-risk group and a low-risk group (Fig. 7).The left side of the dashed line on the X-axis represents the low-risk group, while the right side represents the high-risk group. In this research, Figs. 6 and 7 illustrate, via bar charts, the risk probabilities of the mitotic index predicted for GIST patients based on preoperative CT features. The X-axis represents various patients, while the Y-axis indicates the risk probabilities that patients have GIST with a high mitotic index. The height of each bar corresponds to the predicted probability of a particular patient. We categorized patients into a high-risk group and a low-risk group according to the cut-off value of 0.226. With the nomogram model, we can determine the predicted probability for each patient and compare it with 0.226. If the predicted probability is greater than 0.226, the patient is assigned to the high-risk group; if it is less than or equal to 0.226, the patient is placed in the low-risk group. By comparing the bar charts of the training group (Fig. 6) and the validation group (Fig. 7), we can evaluate whether the prediction performance of the model remains consistent across different datasets. This enables clinicians to make more precise treatment decisions based on the patients' predicted probabilities.

The DCA results for the training group show that this Nomogram provides clinical net benefit when the risk threshold is between 0.07 and 0.93 (Fig. 8). Similarly, the DCA analysis for the validation group indicates that the Nomogram provides clinical net benefit within a risk threshold range of 0.15 to 0.93 (Fig. 8). In summary, most of the curve of the model stays far away from the two extreme curves, indicating a relatively large range of probability within the appliable domain. This suggests that the prediction model has strong clinical practicality.

Discussion

This research has identified and utilized three key indicators—tumor size, liquefaction/necrosis, and morphological characteristics—from a multitude of imaging features to develop and validate a Nomogram model for predicting mitotic index. The model has exhibited robust predictive capabilities, precision, and clinical applicability, offering a visually intuitive and highly valuable guidance instrument for assessing the risk of GIST utilizing preoperative CT features in clinical practice.

The mitotic index is the primary factor in assessing the risk of recurrence for GIST[8]. Xu et al.[14] demonstrated that the mitotic count serves as a significant monitoring tool within 5 years post-surgery for GIST recurrence and in identifying high-risk patients, thereby functioning as a predictive factor for the stability of GIST. Although the majority of GIST cases measuring less than 5 cm are generally considered benign, there is a notable minority that poses a substantial risk of malignancy, particularly those displaying a mitotic index exceeding 5 or 10 per high-
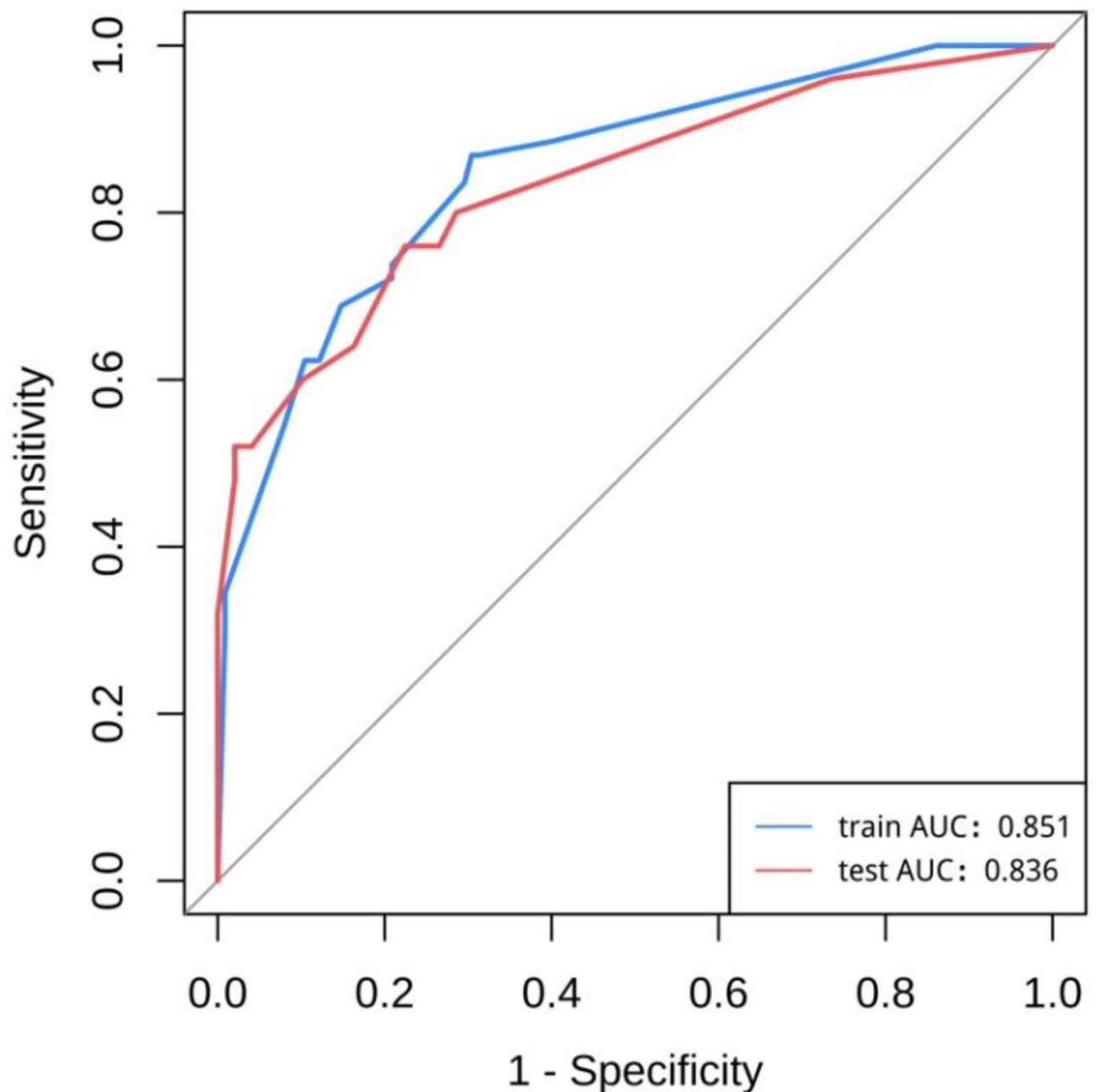
Fig. 3. ROC of the Nomogram prediction model.

power field (HPF). The preoperative detection of such cases often poses a significant challenge[15,16]. According to the AFIP criteria, the recurrence or metastasis of GIST measuring 2–5 cm is primarily determined by the mitotic index Specifically, a high mitotic index (> 5/50HPF) increases the risk by a factor of 10 compared to a low mitotic index (≤ 5/50HPF)[17]. Furthermore, NIH has explicitly designated the mitotic index as an essential component in the assessment of GIST risk, stipulating that a mitotic index greater than 5 signifies a heightened aggressiveness in tumor behavior[18]. This underscores the paramount importance of accurate mitotic count assessment in facilitating the formulation of precise and individualized treatment plans by physicians. At present, B-mode ultrasound and CT scans, as common imaging techniques for abdominal examinations, each have their unique advantages. B-mode ultrasound is cost-effective, allows for dynamic observation, and is highly portable. However, when observing GIST, ultrasound is highly susceptible to interference from factors such as intestinal gas. As a result, its ability to clearly present the overall morphology, precise location of the tumor, and its relationship with surrounding tissues may be inferior to that of CT scans. Precisely for this reason, both at home and abroad, CT scans are recommended as the preferred routine examination for GIST. In this study, the mitotic index of GIST was accurately predicted based on preoperative CT features. This not only promotes the

B= 1000 repetitions, boot   Mean absolute error=0.036 n=176
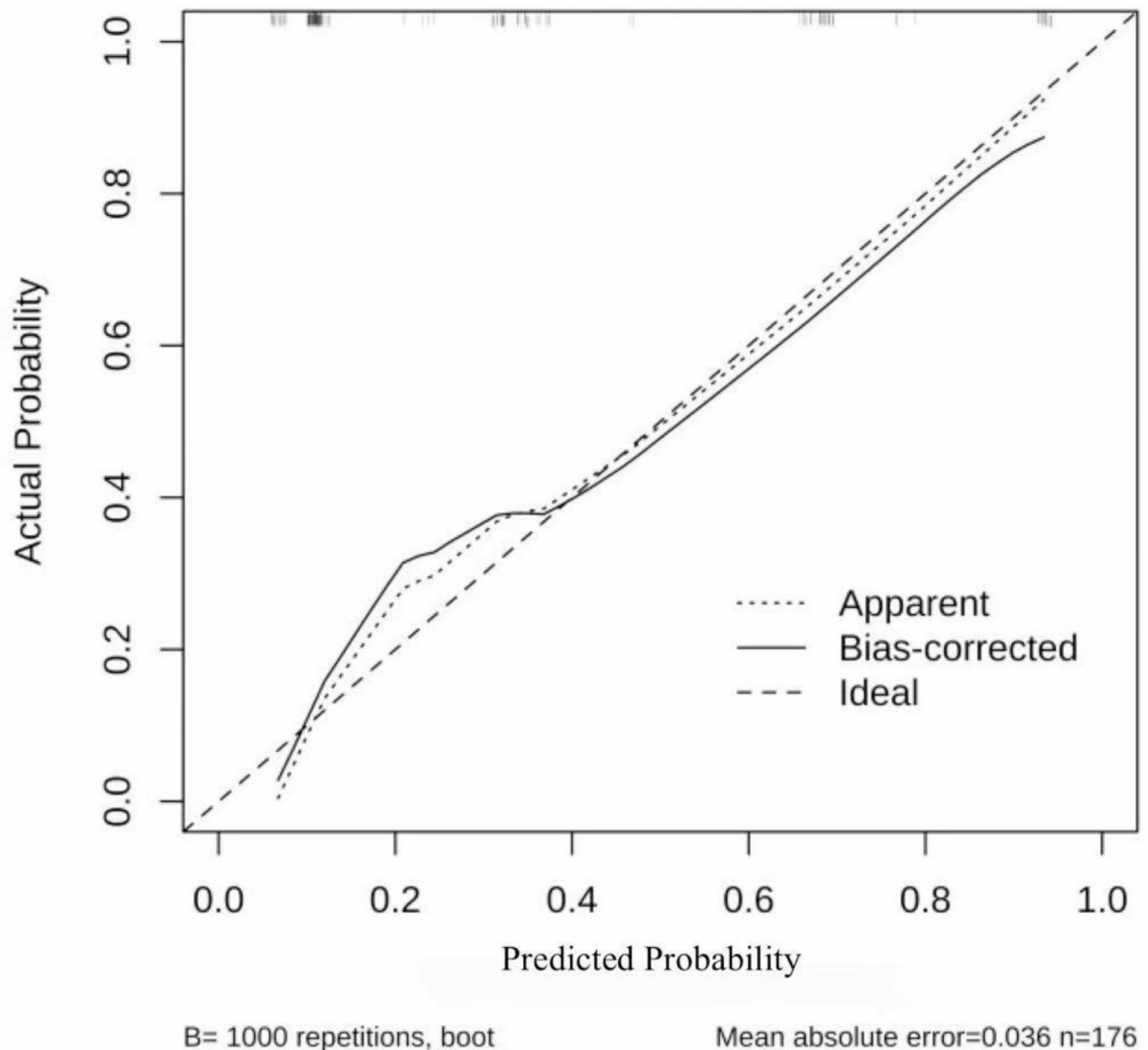
Fig. 4. Calibration curve of the Nomogram prediction model for the training group.

progress of non-invasive imaging examinations replacing invasive needle biopsies but also holds promise as a new assessment tool for grading the risk of GIST.

This study has revealed that tumor size, liquefaction/necrosis, and morphological characteristics are independent risk factors for a high mitotic index in GIST. Mazzei et al.[18] discovered that GISTs characterized by a high mitotic index consistently manifest with a larger maximum diameter in comparison to those with a low mitotic index, indicating a positive correlation between the size of GIST and its degree of malignancy. Additionally, the NIH has incorporated GIST tumor size as a fundamental element in risk stratification, with larger tumors indicating a higher degree of malignancy. This finding aligns with the observations presented in this study. Grazzini et al.[19] identified necrosis as a predictive factor for recurrence risk in GIST based on CT characteristics, achieving a remarkable accuracy rate of 89.3%. Ren et al.[20] likewise demonstrated that necrosis in GIST serves as a predictor of malignant behavior, which concurs with the findings of the present study. Chen et al.[21] found that the morphological characteristics of GIST observed on CT scans possess significant predictive value for mitotic index ($P < 0.05$). Wei et al.[22] quantitatively analyzed the morphological features of GIST and discovered a significant correlation between these features and risk levels ($P < 0.05$). Specifically, tumors with more irregular shapes were predictive of poorer prognosis and higher recurrence rates, which is consistent with the findings of this study.

In this study, tumor location, border, calcification, growth pattern, and ulceration were not identified as independent risk factors for a high mitotic index in GIST. The results of Zheng et al.[23] are congruent with the present study, indicating that tumor location does not significantly impact the risk of GIST ($P > 0.05$).
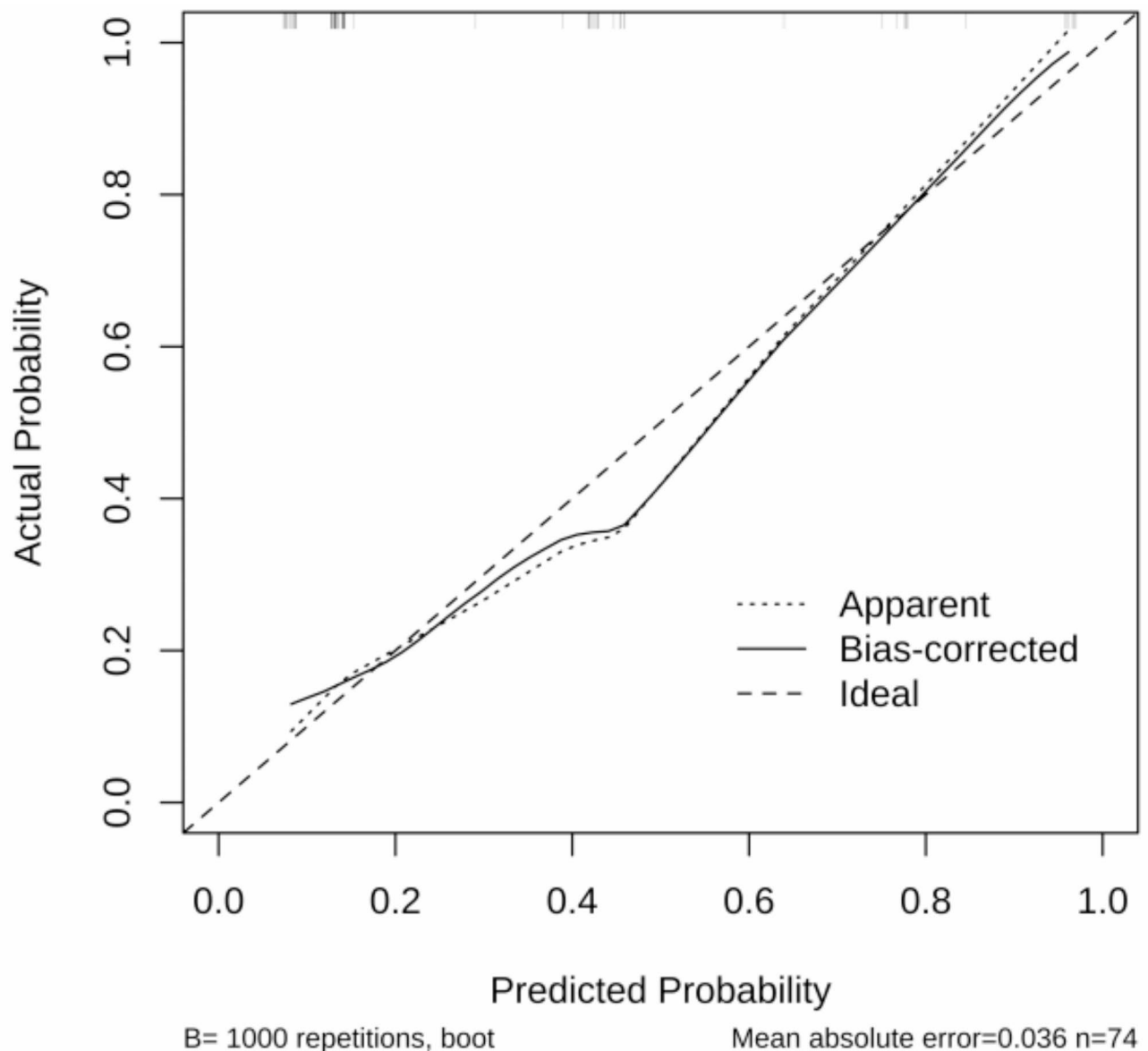
Fig. 5. Calibration curve of the Nomogram prediction model for the validation group.

Conversely, Miettinen et al.[24] have reported that tumor location is a pivotal factor in predicting recurrence and malignancy, with non-gastric GISTs exhibiting a higher degree of malignancy, even when considering tumors of similar size and mitotic index. Burkill et al.[25] observed that the majority (86%) of malignant GISTs display clear borders. In contrast, Jung et al.[4], through a retrospective analysis of 113 patients who underwent radical resection for GIST, reported that an unclear border (OR = 4.93, P = 0.023) was an independent predictor of postoperative recurrence. The author believes that the reasons for such differences may involve multiple aspects: (1) Sample size and individual differences significantly affect the stability of research results. Specifically, the volume of samples included in the study, genetic background variations among patients, and differences in geographical distribution can all be important factors contributing to result discrepancies, undoubtedly increasing the complexity and challenge of assessment. (2) In research on GIST, the definition of tumor boundaries also exhibits diversity. For instance, this paper adopts tumor clarity as the assessment criterion, while some studies may focus on the regularity of tumor morphological features. Such differences in definitions are likely to impact the accurate assessment of independent risk factors for high mitotic index in GIST. Additionally, the identification of boundaries is also influenced by the subjective judgments of radiological physicians, further increasing the uncertainty of assessment. The research conducted by Jia et al.[26] revealed that radiological features such as calcification and ulceration were correlated with the risk stratification of GISTs of 1–2 cm (P < 0.05), which is different from the findings of this study. In summary, the predictive effect of tumor location, margin, calcification, growth pattern, and ulceration on the mitotic index of GISTs remains controversial and requires further validation through large-sample, multicenter studies.
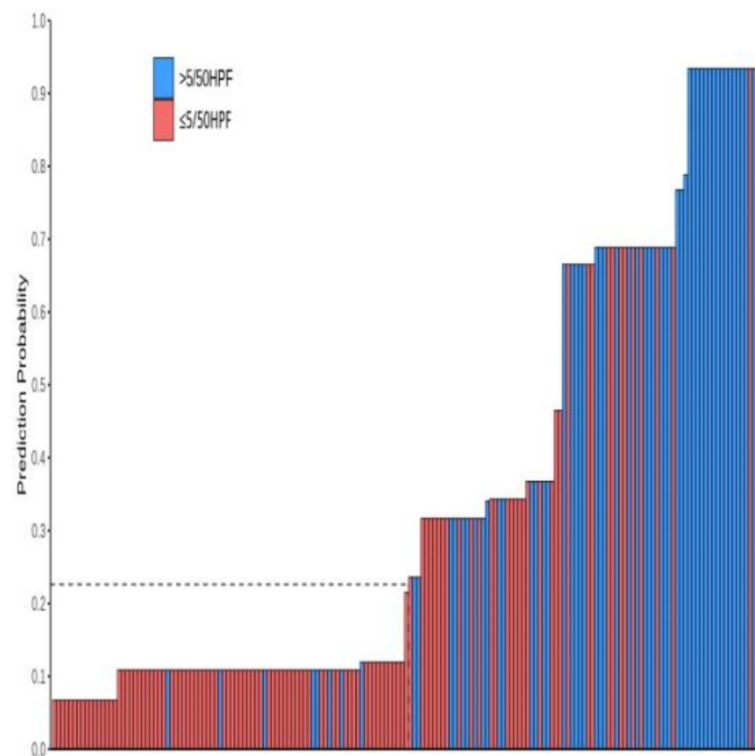
Fig. 6. Bar chart of risk stratification based on the prediction model for the training group.
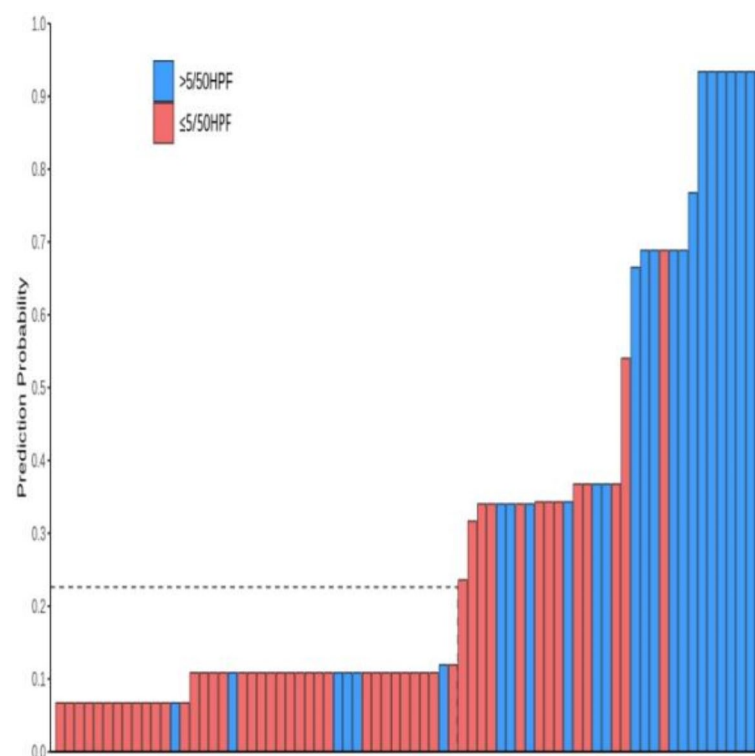
Fig. 7. Bar chart of risk stratification based on the prediction model for the validation group.
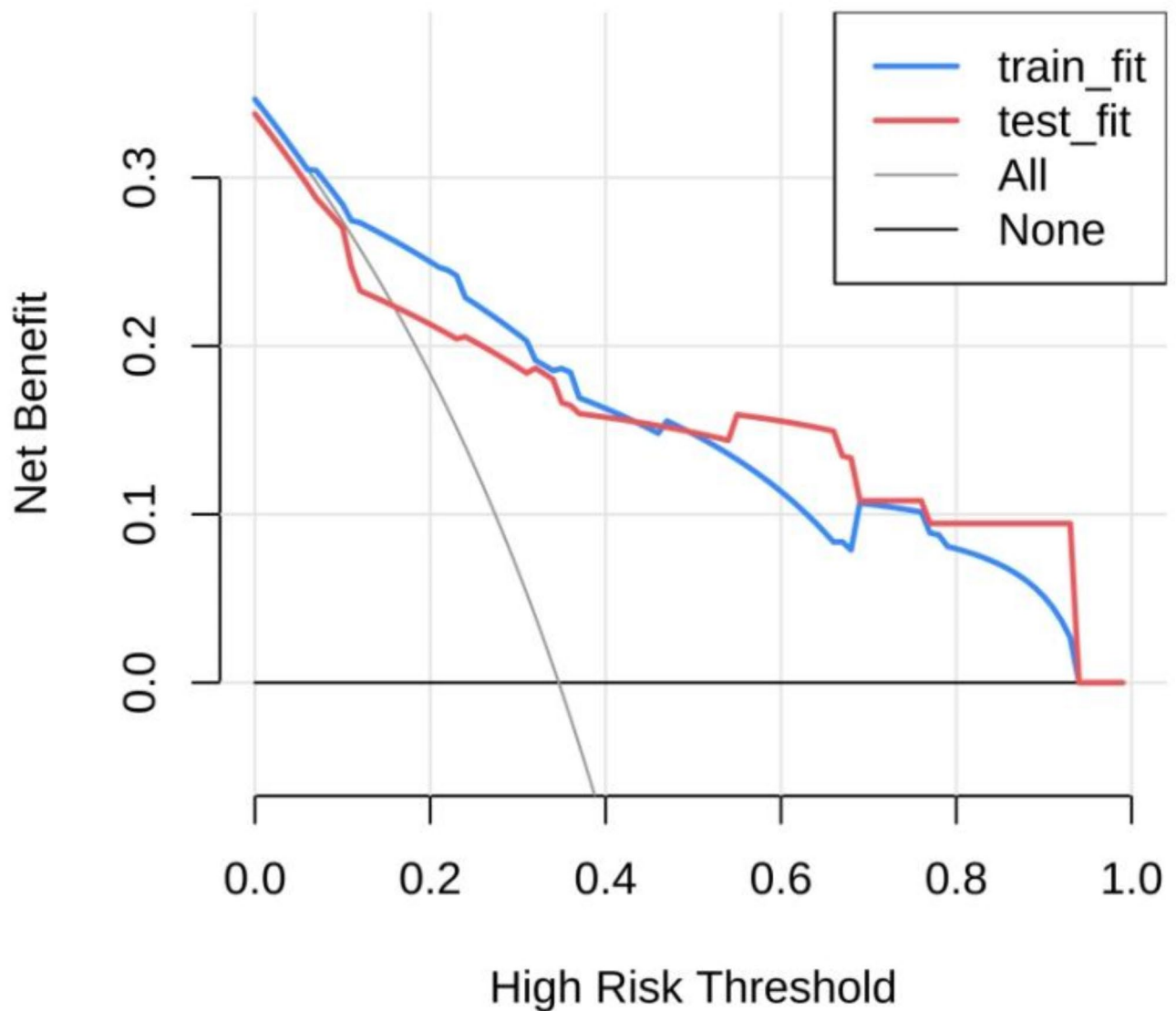
Fig. 8. DCA for the Nomogram prediction model.

There are certain limitations in this study: (1) As a retrospective study, there may be potential for selection bias; (2) Being a single-center study with a relatively small sample size, the model validation was limited to internal validation only. Further external validation using multi-center, large-sample data is needed to confirm the accuracy of the model. In addition, in future research, we can combine preoperative CT features with the gene mutation status to construct a more comprehensive prediction model. Preoperative CT provides the macroscopic manifestations of GIST, such as tumor size, liquefaction/necrosis, and morphological characteristics. The gene mutation status, on the other hand, reveals, at the molecular level, the mutation types, disease malignancy, invasiveness, etc. of GIST, providing a more accurate and effective basis for personalized treatment of patients.

Conclusion

In summary, the nomogram model constructed in this study, based on three CT features including tumor size, liquefaction/necrosis, and morphological characteristics, can effectively assess the mitotic index of GIST patients before surgery. This allows for accurate preoperative risk stratification and provides guidance for personalized treatment plans, such as selecting appropriate surgical approaches and determining the need for neoadjuvant chemotherapy. It aids in reducing the reliance on preoperative puncture biopsy and decreases the risk of tumor rupture and dissemination. Additionally, it assists doctors in identifying patients who may benefit from neoadjuvant therapy, improving surgical success rates and reducing postoperative risks.

Data availability

All data generated or analyzed during this study are included in this published article. And the primary data could be achieved from the corresponding author.

References

1. Li, J. et al. Efficacy and safety of endoscopic resection for gastric Gastrointestinal stromal tumors originating from the muscularis propria. *Dig. Dis. Sci.* (2024).
2. Blay, J-Y. et al. Gastrointestinal stromal tumours. *Nat. Rev. Dis. Prim.* **7**(1), 1–22. https://doi.org/10.1038/s41572-021-00254-5 (2021).
3. Anonymous. Identification and validation of protein biomarkers for predicting Gastrointestinal stromal tumor recurrence. *Comput. Struct. Biotechnol. J.* **23**, 1065–1075. https://doi.org/10.1016/j.csbj.2024.02.017 (2024).
4. Casali, P. G. et al. Gastrointestinal stromal tumours: esmo-euracan-genturis clinical practice guidelines for diagnosis, treatment and follow-up. *Ann. Oncol.* **33**(1), 20–33. https://doi.org/10.1016/j.annonc.2021.09.005 (2022).
5. Liu, D-N. et al. Cytoreductive surgery offers prognostic benefits in metastatic Gastrointestinal stromal tumors with generalized progression following Imatinib therapy: A single Institute retrospective study. *BMC Surg.* **23**(1), 1–9. https://doi.org/10.1186/s12893-023-02087-3 (2023).
6. Van Der Burg, S. J. C. et al. Neoadjuvant Imatinib in locally advanced Gastrointestinal stromal tumors (gists) is effective and safe: Results from a prospective single-center study with 108 patients. *Ann. Surg. Oncol.* **30**(13), 8660–8668. https://doi.org/10.1245/s10434-023-14346-x (2023).
7. Galluzzo, A. et al. Radiomics in Gastrointestinal stromal tumours: An up-to-date review. *Jpn. J. Radiol.* **41**(10), 1051–1061. https://doi.org/10.1007/s11604-023-01441-y (2023).
8. Nishida, T. et al. Clinical importance of tumor rupture in Gastrointestinal stromal tumor. *J. Dig. Dis.* https://doi.org/10.1111/1751-2980.13190 (2023).
9. Hølmebakk, T. et al. Integrating anatomical, molecular and clinical risk factors in Gastrointestinal stromal tumor of the stomach. *Ann. Surg. Oncol.* **28**(11), 6837–6845. https://doi.org/10.1245/s10434-021-09605-8 (2021).
10. Gao, J. et al. Follow-up analysis and research of very low-risk and low-risk Gastrointestinal stromal tumors after endoscopic resection. *Sci. Rep.* **14**(1), 17872. https://doi.org/10.1038/s41598-024-68460-1 (2024).
11. Judson, I. et al. Gastrointestinal stromal tumour (gist): British sarcoma group clinical practice guidelines. *Br. J. Cancer* 1–10. https://doi.org/10.1038/s41416-024-02672-0 (2024).
12. Chen, T. et al. Comparison of modified Nih and Afip risk-stratification criteria for Gastrointestinal stromal tumors: A multicenter retrospective study. *Zhonghua Wei Chang Wai Ke Za Zhi = Chin. J. Gastrointest. Surg.* **20**(9), 1020–1024 (2017).
13. Lin, J-X. et al. Prediction of the mitotic index and preoperative risk stratification of Gastrointestinal stromal tumors with Ct radiomic features. *Radiol. Med.* **128**(6), 644–654. https://doi.org/10.1007/s11547-023-01637-2 (2023).
14. Xu, S-J. et al. Dynamic survival analysis of Gastrointestinal stromal tumors (gists): A 10-year follow-up based on conditional survival. *BMC Cancer* **21**(1), 1170. https://doi.org/10.1186/s12885-021-08828-y (2021).
15. Xu, J. et al. A multi-class scoring system based on Ct features for preoperative prediction in gastric Gastrointestinal stromal tumors. *Am. J. Cancer Res.* **10**(11), 3867–3881 (2020).
16. Zhang, X. et al. Gastrointestinal stromal tumor risk classification: Spectral Ct quantitative parameters. *Abdom. Radiol.* **44**(7), 2329–2336. https://doi.org/10.1007/s00261-019-01973-w (2019).
17. Seven, G., Arici, D. S. & Senturk, H. Correlation of endoscopic ultrasonography features with the mitotic index in 2- to 5-cm gastric Gastrointestinal stromal tumors. *Dig. Dis.* **40**(1), 14–22. https://doi.org/10.1159/000516250 (2022).
18. Mazzei, M. A. et al. Gastrointestinal stromal tumors (gist): A proposal of a ct-based predictive model of Miettinen index in predicting the risk of malignancy. *Abdom. Radiol.* **45**(10), 2989–2996. https://doi.org/10.1007/s00261-019-02209-7 (2020).
19. Grazzini, G. et al. Gastrointestinal stromal tumors: Relationship between preoperative Ct features and pathologic risk stratification. *Tumori* **107**(6), 556–563. https://doi.org/10.1177/0300891621996447 (2021).
20. Ren, C., Wang, S. & Zhang, S. Development and validation of a nomogram based on Ct images and 3d texture analysis for preoperative prediction of the malignant potential in Gastrointestinal stromal tumors. *Cancer Imaging* **20**(1), 5. https://doi.org/10.1186/s40644-019-0284-7 (2020).
21. Chen, T. et al. The roles of Ct and Eus in the preoperative evaluation of gastric Gastrointestinal stromal tumors larger than 2 cm. *Eur. Radiol.* **29**(5), 2481–2489. https://doi.org/10.1007/s00330-018-5945-6 (2019).
22. Wei, S-C. et al. Risk stratification in gist: Shape quantification with Ct is a predictive factor. *Eur. Radiol.* **30**(4), 1856–1865. https://doi.org/10.1007/s00330-019-06561-6 (2020).
23. Zheng, T. et al. Evaluation of risk classifications for Gastrointestinal stromal tumor using multi-parameter magnetic resonance analysis. *Abdom. Radiol.* **46**(4), 1506–1518. https://doi.org/10.1007/s00261-020-02813-y (2021).
24. Miettinen, M. & Lasota, J. Gastrointestinal stromal tumors: Review on morphology, molecular pathology, prognosis, and differential diagnosis. *Arch. Pathol. Lab. Med.* **130**(10), 1466–1478. https://doi.org/10.5858/2006-130-1466-GSTROM (2006).
25. Burkill, G. J. C. et al. Malignant Gastrointestinal stromal tumor: distribution, imaging features, and pattern of metastatic spread. *Radiology* **226**(2), 527–532. https://doi.org/10.1148/radiol.2262011880 (2003).
26. Jia, X. et al. Risk stratification for 1- to 2-cm gastric Gastrointestinal stromal tumors: Visual assessment of Ct and Eus high-risk features versus Ct radiomics analysis. *Eur. Radiol.* **33**(4), 2768–2778. https://doi.org/10.1007/s00330-022-09228-x (2023).

Acknowledgements

Author contributions

Conceptualization, R.Y.; methodology, R.Y. and Y.Y.; validation, R.Y., J.L., Y.Y. and D.Y.; formal analysis, R.Y., J.L., Y.Y. and A.J.; investigation, R.Y.; data curation, R.Y. and Y.Y.; writing-original draft preparation, R.Y., Y.Y., A.J. and D.Y.; writing-review and editing, R.Y.; supervision, D.Y. All authors have read and agreed to the published version of the manuscript.

Declarations

Competing interests

The authors declare no competing interests.

Additional information

Correspondence and requests for materials should be addressed to D.Y.